ELSEVIER

Contents lists available at ScienceDirect

Experimental Eye Research

journal homepage: www.elsevier.com/locate/yexer



670nm light treatment following retinal injury modulates Müller cell gliosis: Evidence from *in vivo* and *in vitro* stress models



Yen-Zhen Lu^a, Nilisha Fernando^a, Riccardo Natoli^{a,b}, Michele Madigan^{c,d}, Krisztina Valter^{a,b,*}

- ^a The John Curtin School of Medical Research, The Australian National University, Canberra, ACT, Australia
- ^b Medical School, The Australian National University, Canberra, ACT, Australia
- ^c Save Sight Institute, Discipline of Clinical Ophthalmology, The University of Sydney, Sydney, NSW, Australia
- d School of Optometry and Vision Science, The University of New South Wales, Kensington, NSW, Australia

ARTICLE INFO

Keywords: Müller cell Gliosis Retinal degeneration 670 nm light Inflammation

ABSTRACT

Photobiomodulation (PBM) with 670 nm light has been shown to accelerate wound healing in soft tissue injuries, and also to protect neuronal tissues. However, little data exist on its effects on the non-neuronal components of the retina, such as Müller cells (MCs), which are the principal macroglia of the retina that play a role in maintaining retinal homeostasis. The aim of this study was to explore the effects of 670 nm light on activated MCs using *in vivo* and *in vitro* stress models. Adult Sprague-Dawley rats were exposed to photo-oxidative damage (PD) for 24 h and treated with 670 nm light at 0, 3 and 14 days after PD. Tissue was collected at 30 days post-PD for analysis. Using the *in vitro* scratch model with a human MC line (MIO-M1), area coverage and cellular stress were analysed following treatment with 670 nm light. We showed that early treatment with 670 nm light after PD reduced MC activation, lowering the retinal expression of GFAP and FGF-2. 670 nm light treatment mitigated the production of MC-related pro-inflammatory cytokines (including IL-1β), and reduced microglia/macrophage (MG/MΦ) recruitment into the outer retina following PD. This subsequently decreased photoreceptor loss, slowing the progression of retinal degeneration. *In vitro*, we showed that 670 nm light directly modulated MC activation, reducing rates of area coverage by suppressing cellular proliferation and spreading. This study indicates that 670 nm light treatment post-injury may have therapeutic benefit when administered shortly after retinal damage, and could be useful for retinal degenerations where MC gliosis is a feature of disease progression.

1. Introduction

Müller cells (MCs) are the principal macroglia of the vertebrate retina and play a key role in maintaining retinal structure and homeostasis. During retinal injury, the early response of MCs involves the release of neuroprotective factors such as ciliary neurotrophic factor (CNTF), and fibroblast growth factor (FGF-2) (Bringmann and Wiedemann, 2012; Shen et al., 2012), which have been shown to rescue photoreceptors following photo-oxidative damage (Valter et al., 2005). Activated MCs express chemokine C-C motif ligand 2 (CCL2), a known chemoattractant and activator for MG/MΦ *in vitro* (Matsushima et al., 1989; Nakazawa et al., 2007a; Yoshimura et al., 1989). Exposure to PD *in vivo* induces retinal *Ccl2* expression in MCs, and subsequent recruitment of MG/MΦ to areas of severe damage (Rutar et al., 2012b). In severe retinal damage, when a large number of neurons are lost, MCs enter into proliferative gliosis forming glial scars (Bringmann et al., 2009), which create barriers that hinder nutrient delivery to surviving

retinal neurons, causing further cell death leading to disease progression (Albarracin and Valter, 2012).

PBM is low-energy photo-irradiation that has been shown to accelerate wound healing in skin (Conlan et al., 1996), mucosa (Desmet et al., 2006), and soft tissue (Herranz-Aparicio et al., 2013). Beneficial effects have also been reported in central nervous system (CNS) tissue injuries involving the spinal cord, retina and optic nerve (Lawrence et al., 2007). Pre-clinical studies in models of retinal degeneration have demonstrated that 670 nm light treatment is neuroprotective, can slow photoreceptor and ganglion cell death (Albarracin et al., 2011, 2013; Eells et al., 2003; Giacci et al., 2014; Natoli et al., 2013; Tang et al., 2013), and reduce pro-inflammatory cytokine secretion, macrophage recruitment and complement activation (Calaza et al., 2015; Kokkinopoulos, 2013; Kokkinopoulos et al., 2013). Acknowledging these benefits, it has recently gained FDA approval for clinical use (Desmet et al., 2006; Fitzgerald et al., 2013; Whelan et al., 2001). Clinical studies over the past decade have further demonstrated the

^{*} Corresponding author. The John Curtin School of Medical Research, Building 131, Garran Rd, The Australian National University, Canberra ACT 2601, Australia. E-mail address: krisztina.valter-kocsi@anu.edu.au (K. Valter).

neuroprotective effect of 670 nm light in retinal degenerations (Ivandic and Ivandic, 2008, 2012; Merry et al., 2017; Tang et al., 2014).

Although the effects of 670 nm light on retinal neurons have been documented, the influence of 670 nm light on non-neuronal cells, including MCs, has not been well-studied. We previously demonstrated that 670 nm light treatment prior to retinal injury could ameliorate the activation of MCs following photo-oxidative damage (Albarracin et al., 2011; Albarracin and Valter, 2012). However, the effects of administering 670 nm light treatment after photo-oxidative damage have not been fully investigated. In this study, we explored the direct effect of 670 nm light on activated MCs using *in vivo* and *in vitro* models of retinal stress.

2. Materials and methods

2.1. Animals and PD

All experiments were conducted in accordance with the ARVO Statement for the Use of Animals in Ophthalmic and Vision Research and with approval from the Australian National University Animal Experimentation Ethics Committee (A2014/56). Thirty-nine adult albino Sprague-Dawley (SD) rats aged 100–120 postnatal days (P) were used for *in vivo* experiments. Animals were born and raised in low light levels (5 lux) in a 12-h light, 12-h dark cycle with food and water available *ad libitum*. PD was performed as described previously (Albarracin and Valter, 2012). Briefly, animals were exposed to white light (1000 lux) for 24 h using transparent Perspex open-top cages placed under a light source (COLDF2, $2 \times 36W$, IHF; Thorn Lighting, Spennymoor, UK). Animals were returned to a low light environment (5 lux) to recover for 30 days; some animals were treated with 670 nm light during recovery. Animals were euthanized and tissue was collected at 30 days after PD.

2.2. PBM with 670 nm light in vivo

Animals were divided into 5 groups: PD + R0 (PBM commenced immediately after PD, n = 7); PD + R3 (PBM commenced at 3 days after PD, n = 10); PD + R14 (PBM commenced at 14 days after PD, n = 7); PD (animals were exposed to PD only, n = 9); and **control** (animals were not exposed to PD or 670 nm light, n = 6). In the treatment groups (PD + R0, PD + R3, PD + R14) PBM was performed using a 670 nm light-emitting diode array (WARP 75; Quantum Devices, WI, USA) during the period of recovery, commencing at the specified times post-PD. During treatment, animals were positioned so that both eyes were approximately 2.5 cm away from the light source and were exposed to 670 nm light for 3 min at 60 mW/cm², delivering 9J/cm² irradiation to the retina, daily for 5 consecutive days.

2.3. Uniform scratch model using MIO-M1 cells

A spontaneously immortalized human Müller cell line, MIO-M1 (Limb et al., 2002b) was validated for species authenticity (CellBank, Sydney, Australia) and used for *in vitro* experiments. Cells were maintained in Dulbecco's Modified Eagle's Medium (DMEM; Thermo Fisher Scientific, MA, USA) containing 10% fetal bovine serum (FBS, Sigma-Aldrich, MO, USA), supplemented with 6 mM L-glutamine (Thermo Fisher Scientific) in a humidified atmosphere of 5% $\rm CO_2$ at 37 °C. Cells were seeded on 6-well plates ($\rm 1.3 \times 10^5$ per well), on 8-well chamber slides ($\rm 1.3 \times 10^4$ per well) (Millipore, MA, USA), or on transwell inserts (5 µm pore-size; Millipore) (3000/insert) for 2 day at 37 °C in a humidified $\rm CO_2$ incubator to reach 90% confluence. A uniform scratch was created in each well using a 1 ml pipette tip, and a grid was used beneath each well to ensure uniformity between wells. Floating cells and debris were removed by rinsing cells with 0.1M PBS, before wells were replenished with fresh culture growth medium.

To inhibit proliferation, some cells (6-well plates) were incubated

with Mitomycin C (MMC, $10\,\mu\text{g/ml}$, Sigma Aldrich) for $2\,\text{h}$, washed with 0.1M PBS (Arranz-Valsero et al., 2014), and growth medium was replenished prior to the scratch injury.

2.4. 670 nm light treatment in vitro

For PBM of cells, a 670 nm LED array (WARP 10; Quantum Devices) was used. Cells were irradiated 3 times with 670 nm light for 3 min at 60 mW/cm² (9J/cm²). The first PBM treatment was delivered immediately after the scratch, followed by two further irradiations at 4-h intervals in the first 24 h. Four experimental groups were used: nonscratch (NS) control, where cells did not undergo scratch injury or 670 nm treatment; scratch (S), where cells received scratch injury and sham 670 nm treatment (cells underwent identical handling to the 670 nm treatment groups, without the light irradiation); NS+670 and S +670 groups both received 670 nm treatment (N = 3 wells/group, N = 3 repeats). Baseline measurements were taken immediately following the first intervention for each group (scratch \pm 670 nm) – this was designated T = 0. Measurements were performed at T = 24, 48, and 72 h. Digital images of scratch edges were captured using a phasecontrast light microscope (Axiovert 3; Zeiss, Oberkochen, Germany). The progression of cell coverage across the scratch area was analysed by measuring the area covered (pixels) from the edge of the original scratch (T = 0), using ImageJ software (National Institutes of Health, MA, USA).

2.5. Cell migration assay

Cells were seeded on transwell inserts (3000 cells/insert) for analysing cell migration. To initiate migration, serum-free medium was added to the cells on the inserts, while growth medium was added to the lower chamber. After 24, 48 or 72 h, cells on the inserts were fixed with 4% paraformaldehyde for 10 min at room temperature, and stained with bisbenzimide (BBZ, 1:10000; Sigma-Aldrich). The non-migrating cells on the surface of the insert membrane were removed using cotton swabs. To measure cell migration across the insert membrane, the number of cells on the lower surface were visualised and counted using a laser-scanning $\rm A1^+$ confocal microscope (Nikon, Tokyo, Japan) (Lu et al., 2013).

2.6. Flow cytometry analysis for cell viability and cell cycle

Flow cytometry was used to assess cell cycle status and cell death. Vybrant DyeCycle Violet Stain (Thermo Fisher Scientific) was utilized to recognize live cells, and 7-aminoactinomycin D (7-AAD, Thermo Fisher Scientific) was used to identify dead cells. Briefly, cells were trypsinized and collected from 6-well plates. Cells were incubated with $1\,\mu l$ of Vybrant DyeCycle Violet Stain diluted in 1 ml Hank's Balanced Salt Solution (HBSS, Thermo Fisher Scientific) for 2 h at 37 °C in the dark, and then was rinsed twice with 0.1M PBS. Cell pellets were resuspended in HBSS containing 2.5% 7-AAD and were incubated for 10 min at 37 °C in the dark. Fluorescence was detected using flow cytometry (LSRII; BD, CA, USA) and analysed using FlowJo (FlowJo, OR, USA).

2.7. Immunofluorescent staining on retinal tissues and cells

Following 30 days recovery, animals were euthanized using an intraperitoneal injection of barbiturate (Valabarb; Virbac, NSW, Australia). One eye of each animal was enucleated, immersion fixed in 4% paraformaldehyde and then cryoprotected with 15% sucrose overnight. Eyes were cryosectioned at 16 µm thickness. Immunofluorescent staining was performed as previously described (Albarracin et al., 2011; Albarracin and Valter, 2012), using primary antibodies listed in Table 1. Following incubation with a fluorophore-conjugated secondary antibody, the cell nuclei were stained with bisbenzimide. To quantify

Table 1
Primary antibodies used for immunostaining.

Primary antibody	Source	Catalog number	Host species	Dilution factor
FGF-2	Millipore	05–118	Mouse	1:200
GFAP (retinas)	Dako	Z0334	Rabbit	1:400
GFAP (cells)	Thermo Fisher Scientific	MS1376	Mouse	1:200
Iba1	Wako	019-19741	Rabbit	1:500
Ki67	Millipore	AB9260	Rabbit	1:300
Recoverin	Millipore	AB5585	Rabbit	1:200
Vimentin	Sigma-Aldrich	V6630	Mouse	1:150

photoreceptor cell survival in the retina, the number of photoreceptor cell rows in the ONL was counted as detailed previously (Fernando et al., 2016). Immunofluorescence was visualised using the laser-scanning ${\rm A1}^+$ confocal microscope and acquired using NIS-Element AR software (Nikon). Images were processed using Photoshop CS6 software (Adobe Systems, CA, USA).

MIO-MI cells seeded in 8-well chamber slides (Millipore) were fixed with 2% paraformaldehyde for 30 min, and stained following the protocol described previously (Lu et al., 2017). For analysis of cell spreading, cells were incubated in 8-well chamber slides and the cellular cytoskeleton was observed using Vimentin immunostaining (Table 1). The spread of individual cells was measured by calculating the ratio of the area of cell cytoplasm in relation to the area of the nucleus. Cell spreading was quantified by analysing 20–30 cells along the scratch edges in each sample (Lu et al., 2013).

2.8. Quantitative real-time PCR (RT-qPCR)

Retinas were collected and stored in RNA stabilizer (RNAlater; Thermo Fisher Scientific). RNA extraction using an RNAqueous Total RNA isolation kit (Thermo Fisher Scientific) and TRIzol (Thermo Fisher Scientific), as well as cDNA synthesis using a Tetro cDNA Synthesis Kit (Bioline, London, UK) was performed as described previously (Rutar et al., 2011). Gene expression was measured via quantitative real-time polymerase chain reaction (RT-qPCR) using Taqman Gene Expression Master Mix (Thermo Fisher Scientific) and commercially available Taqman hydrolysis probes (Table 2, Thermo Fisher Scientific), according to previously described methodology (Rutar et al., 2011). Each sample was run in duplicate on the QuantStudio Flex 12K instrument (Thermo Fisher Scientific). Analysis was performed using the comparative cycle threshold method ($^{\Delta C}$ _t), with target gene expression normalised to the expression of the reference gene, glyceraldehyde 3-phosphate dehydrogenase (*Gapdh*).

2.9. Statistical analysis

Data were analysed with a one-way analysis of variance (ANOVA), with Tukey's multiple comparisons post-hoc test. Data were reported as mean \pm SEM, and values of P < .05 were considered to be statistically significant. All statistical analyses were performed using Prism 6

Table 2
Taqman hydrolysis probes used for qPCR.

Gene Symbol	Source	Catalog number	Host species
Casp8	Caspase 8	Rn00574069_m1	64044
Ccl2	Chemokine (C-C motif) ligand 2	Rn01456716_g1	24770
Fgf-2	Fibroblast growth factor 2	Rn00570809_m1	54250
Gfap	Glial fibrillary acidic protein	Rn00566603_m1	24387
Gapdh	Glyceraldehyde-3-phosphate dehydrogenase	Rn99999916_s1	24383
Π-1β	Interleukin 1 beta	Rn00580432_m1	24494

(GraphPad, CA, USA).

3. Results

3.1. Early treatment with 670 nm light reduced photoreceptor loss following photo-oxidative damage

Recoverin labelling showed a disruption of photoreceptor (PR) structures following PD. At the lesion site, the ONL was largely obliterated centrally, while on the periphery of the lesion ONL was present but severely distorted, the remaining PRs were scattered and their inner and outer segments were absent (Fig. 1E and F left). At the penumbra of the lesion, the ONL was more compact, and inner and outer segments were observed (Fig. 1E, F right). The presence or absence of IS/OS and the organisation of the ONL were used to define the edge of the lesion (dotted lines in Fig. 1F). A similar pattern of photoreceptor damage was found in the lesion and penumbra of PD + R0 (Fig. 1H and I), PD + R3 (Fig. 1K and L), and PD + R14 (Fig. 1N, O) retinas, suggesting that the 670 nm light cannot restore photoreceptor structural damage.

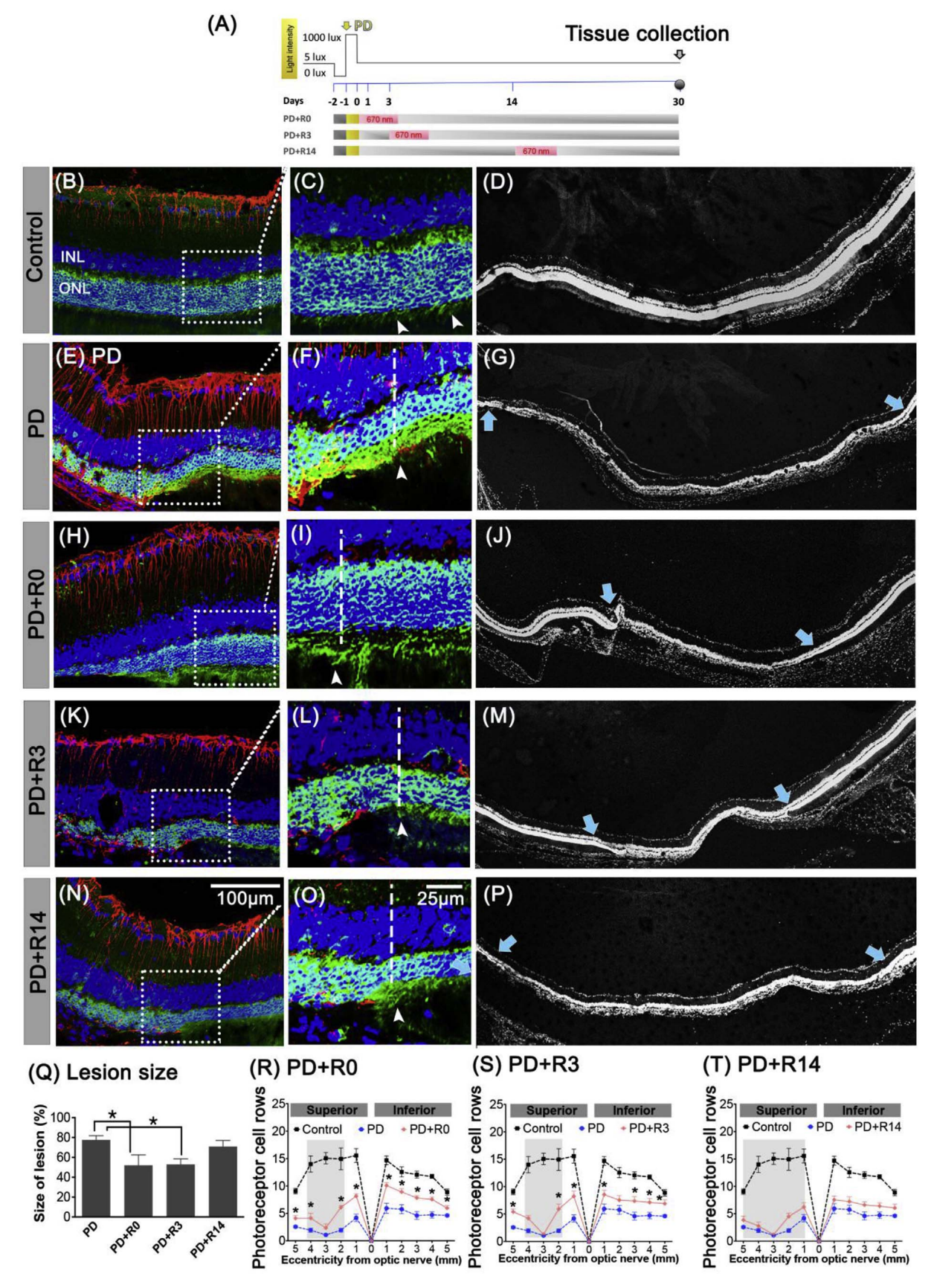
We have previously shown that following PD, there is a focal loss of photoreceptors in the superior retina, which becomes the centre of a progressive lesion, which may engulf the entire retina over time (Rutar et al., 2010). To assess whether 670 nm light had an effect on lesion expansion, we measured the size of the lesion along the retina at 30 days following PD, using the criteria to define the edge of lesion, as described above. In control retinas, no lesion was detected (Fig. 1D). In the PD group, approximately 80% of the superior retina displayed photoreceptor loss indicating an expansive field of lesion (Fig. 1G, Q). Early treatment with 670 nm light (PD + R0 and PD + R3), resulted in a significant reduction in lesion size (P < .05), affecting approximately half of the superior retina only (Fig. 1J, M, Q). Treatment at 14 days following PD (PD + R14) resulted in no significant change in lesion size compared to PD only retinas (Fig. 1P, Q).

PD caused a significant reduction in ONL thickness along the retina, quantified by the number of photoreceptor cell rows (Fig. 1R–T blue lines). Following treatment with 670 nm light, retinas treated immediately (PD + R0, Fig. 1R) and at 3 days after PD (PD + R3, Fig. 1S) had a significant protection against photoreceptor loss along the majority of the retina compared to PD only retinas (P < .05). 670 nm light treatment commencing at 14 days post-PD (PD + R14) resulted in no significant difference in the number of photoreceptor cell rows compared to PD only retinas (Fig. 1T).

3.2. Treatment with 670 nm light reduced Müller cell gliosis

To assess MC structural changes, we used Vimentin immunolabelling, a cytoskeletal protein marker. It showed thickened MC process that surrounded the surviving PRs in the area of the lesion (yellow color in Fig. 1F), indicating glial scar formation in the ONL. Co-localisation of Recoverin and Vimentin fluorescence was barely present in the 670 nm light-treated retinas (Fig. 1I, L, O).

To measure retinal stress, GFAP protein expression was assessed via immunohistochemistry. In control retinas GFAP was only expressed by astrocytes (Fig. 2A). Following PD, GFAP labelling was present in MCs, expanding the entire length of the inner and outer processes of the cells in the area of lesion (Fig. 2B). Treatment with 670 nm light modified GFAP expression, as evidenced by the reduced intensity of fluorescence (Fig. 2D, F, H left). At the penumbra, GFAP labelling was still present in MCs, however it did not extend beyond the OPL (Fig. 2D, F, H right). To quantify GFAP expression in the penumbra, we used NIS-Element AR software to measure the intensity of fluorescence along the MCs from GCL to the inner edge of the ONL (Fig. 2C, E, G, I). GFAP labelling was significantly increased in PD retinas compared to controls for almost the entire length of the MCs (Fig. 2C, p < .05). In PD + R0 and PD + R3 retinas the level of GFAP staining in the GCL was not different from those of non-treated PD retinas, indicating that 670 nm irradiation does



(caption on next page)

Fig. 1. 670 nm light treatment on photoreceptor cell death and Müller cell gliosis following photo-oxidative damage (PD). A: Protocol of PD and 670 nm light treatment. B, C, E, F, H, I, K, L, N, O: Sections immunolabelled with Vimentin (red), Recoverin (green) and counterstained with DAPI (blue). Increased presence of Vimentin in MC processes indicate gliosis at the lesion edges. White squares denote the area shown in C, F, I, L, O at higher magnification: White arrowheads indicate photoreceptor IS/OS. White dashed lines denote the border between lesion (on left) and penumbra (right). D, G, J, M, P: ONL lesion size in the superior retina of the control (D), PD (G), PD + R0 (J), PD + R3 (M) and PD + R14 (P). Blue arrows denote the edge of the lesion. Q: Lesion size increases following PD, and is significantly decreased after 670 nm light treatment at 0 and 3 days. R-T: Spider graph showing photoreceptor row numbers along the retinas of control, PD and treated retinas. ONL thickness significantly reduced in all PD retinas, however, they remained significantly thicker at the majority of length of the retina of PD + R0 (R) and PD + R3 (S) animals compared to PD retinas. Grey rectangles in the superior retina denote the lesion area. ONL: outer nuclear layer. INL: inner nuclear layer. All data is presented as the mean \pm SEM. * denotes P < .05 and N = 6-10 for all groups. (For interpretation of the references to color in this figure legend, the reader is referred to the Web version of this article.)

not have an effect on the GFAP expression in the astrocytes. In early-treatment retinas immunostaining of MCs was significantly reduced between the IPL and OPL Fig. 2E, G). Interestingly, in the PD + R14 retinas the entire length of the measured area from GCL to ONL had a significantly reduced immunolabelling compared to PD retinas (Fig. 2I) (p < .05).

Thickened GFAP + MC processes were evident in the outer retina, within and outside of the remnants of ONL at the lesion site following PD (white star, Fig. 2B), suggesting glial scar formation. Such glial scars were not observed outside the lesion area. In retinas irradiated with 670 nm light, GFAP + structures were present in the outer side of the ONL in the area of the lesion however, their staining was much weaker (white starts, Fig. 2D, F, H) than non-treated PD retinas (Fig. 2B).

3.3. Treatment with 670 nm light modified gene expression and microglia presence in the retina

To assess MC activation, we measured the whole retinal expression of *Gfap* and *Fgf-2* genes, which are both expressed by activated MCs, following retinal insult. *Gfap* expression (Fig. 3A) and *Fgf-2* expression (Fig. 3B) were significantly increased at 30 days following PD compared to dim-reared controls (P < .05). *Gfap* expression was significantly reduced in PD + R0 and PD + R3 retinas compared to PD tissue (P < .05, Fig. 3A). *Fgf-2* was significantly reduced in PD + R0 group only when compared to PD retinas (P < .05, Fig. 3B). Late treatment with 670 nm light (PD + R14) had no significant effect on the expression of these two genes.

We investigated the effect of 670 nm light treatment on the expression of inflammatory genes, including the chemokine Ccl2, and

inflammasome components ($\mathit{Il-1\beta}$, $\mathit{Nlrp3}$, $\mathit{Casp8}$). All inflammatory genes assayed were significantly increased (P < .05) following PD compared to controls (Fig. 3C, E and F). Treatment with 670 nm light significantly reduced the expression of inflammasome genes $\mathit{Il-1\beta}$, $\mathit{Nlrp3}$, and $\mathit{Casp8}$ in PD + R0 retinas (P < .05, Fig. 3C, E, F), however did not modulate the expression of these genes in the other treatment groups. Ccl2 gene expression did not increase significantly following PD when compared to controls (Fig. 3D), and though all 670 nm-treated groups showed low levels of expression compared to PD retinas, the differences between the non-treated and treated groups did not reach significance (Fig. 3D).

To determine if 670 nm light had an effect on the recruitment of MG/M Φ to the damaged photoreceptor layer, IBA1 immunohistochemistry was used. In dim-reared control retinas (Fig. 4A), ramified IBA1 + cells were only detected in the inner retina (GCL-OPL). At 30 days following PD, amoeboid IBA1 + microglia were recruited into the outer retina (Fig. 4B). In PD + R0 and PD + R3 groups, the number of activated IBA1 + cells was significantly reduced both in the outer retina and the whole retina compared to PD only retinas (P < .05, Fig. 4C, D, F, G). In the PD + R14 group, there was no significant change in IBA1 + cell recruitment to the retina compared to PD only retinas (Fig. 4E–G).

3.4. Effect of 670 nm light treatment on Müller cell motility and division

To assess MC activation *in vitro*, we used a well-established scratch model using the MIO-M1 cell line (Romo et al., 2011). The rate of area coverage was monitored over $72\,h$ and compared between $670\,nm$ treated and non-treated cells (Fig. 5B–E). We found that $670\,nm$ light

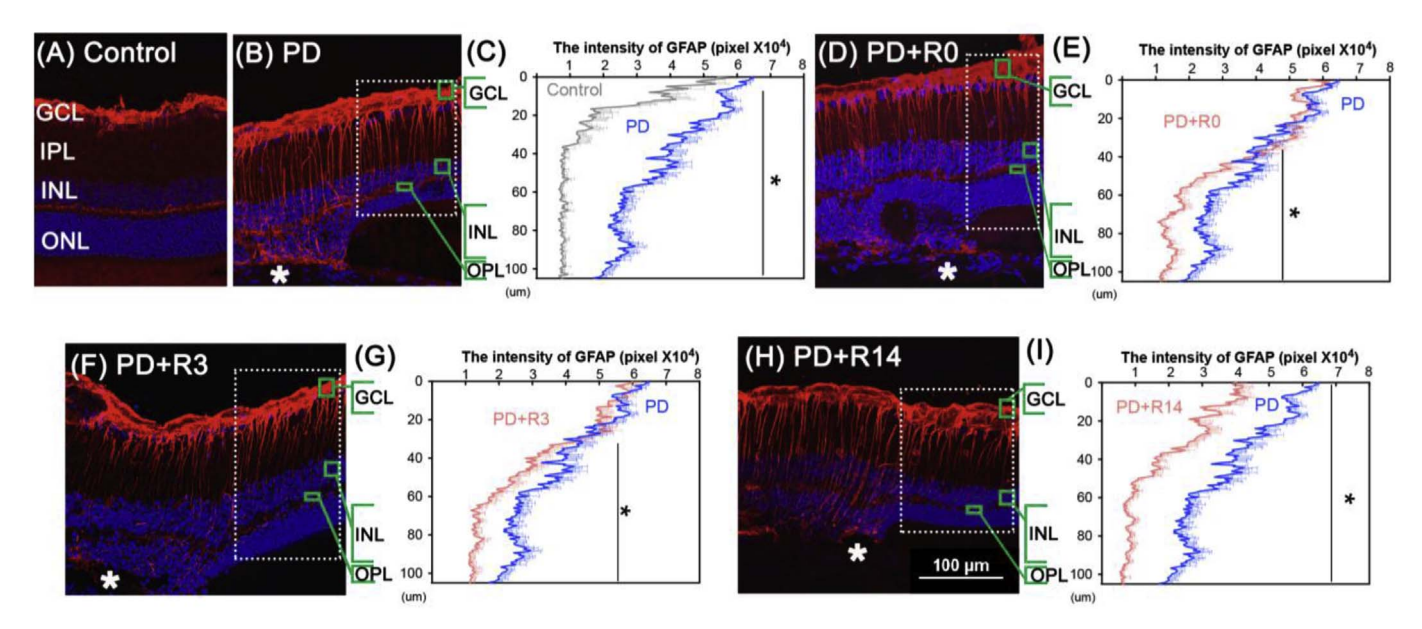


Fig. 2. The effects of 670 nm light treatment on Müller cell gliosis following PD. A, B, D, F, H: Sections immunolabelled with GFAP (red) show that in control retinas only astrocytes are labeled, while MCs become GFAP + after PD indicating tissue stress. White * denotes glial scars in and outside of the ONL in the lesion area. C, E, G, I: The GFAP intensity profile across Müller cell processes in the penumbra adjoining the lesion (white boxes). GCL: ganglion cell layer. INL: inner nuclear layer. OPL: outer plexiform layer. All data is presented as the mean + SEM. * (Black) denotes P < .05 and N = 6–10 for all groups. (For interpretation of the references to color in this figure legend, the reader is referred to the Web version of this article.)

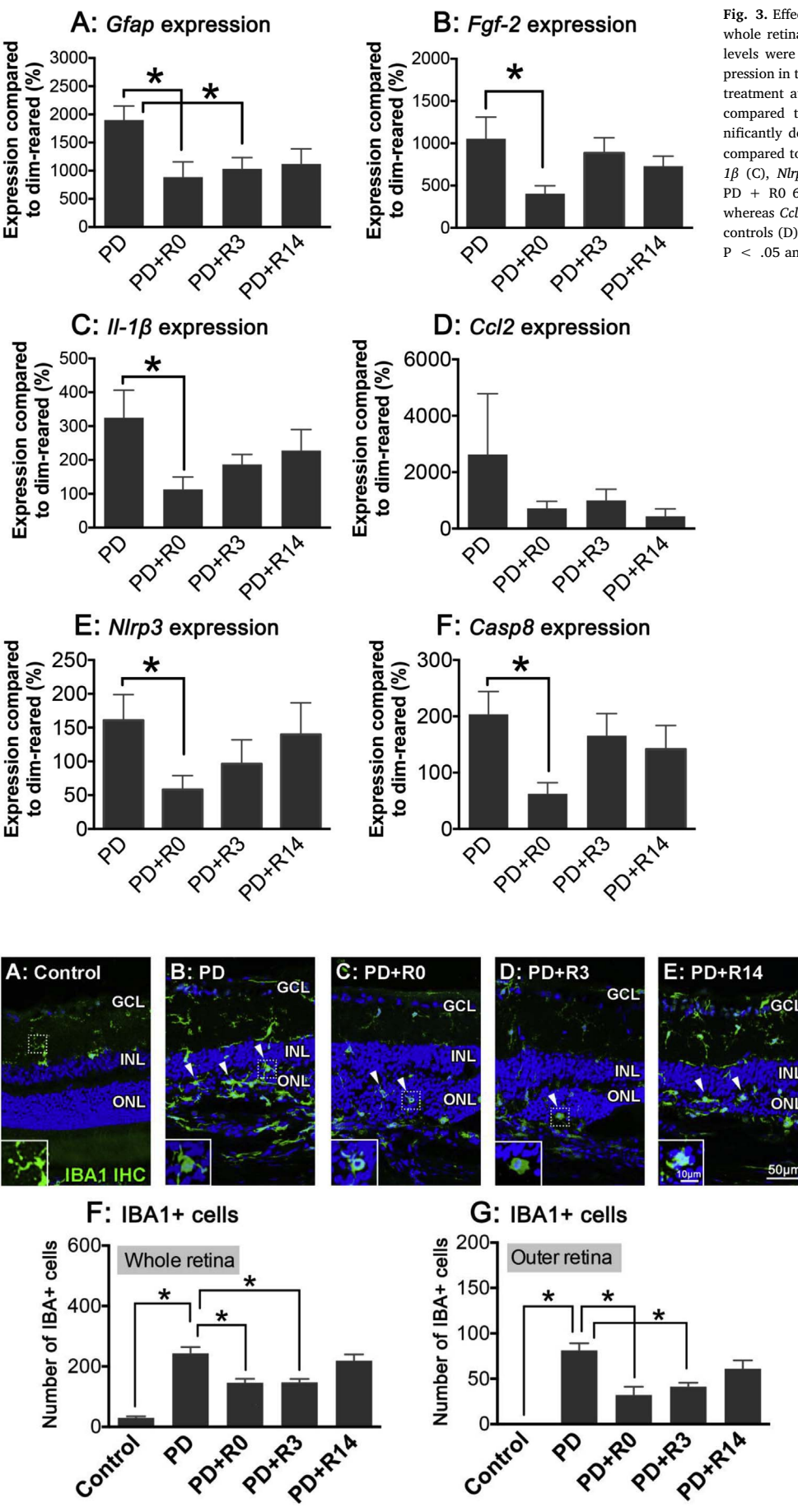


Fig. 3. Effects of 670 nm light treatment on gene expression in whole retinas following photo-oxidative damage (PD). Expression levels were compared to dim-reared control retinas. **A:** *Gfap* expression in the retina was significantly decreased after 670 nm light treatment at 0 (PD + R0) and 3 days (PD + R3) following PD, compared to non-treated PD controls. **B:** *Fgf-2* expression significantly decreased in the PD + R0 670 nm light-treated group compared to PD controls. **C-F:** Inflammatory gene expression of $\mathit{Il-1\beta}$ (C), $\mathit{Nlrp3}$ (E), and $\mathit{Casp8}$ (F) decreased significantly in the PD + R0 670 nm light-treated group compared to PD controls, whereas $\mathit{Cel2}$ expression did not significantly change compared to controls (D). All data is presented as the mean \pm SEM. * denotes P < .05 and N = 6-10 for all groups.

Fig. 4. Effects of 670 nm light on microglia and macrophage recruitment following photo-oxidative damage (PD). A-E: Representative images of the superior retina show that IBA1 + cells (green) are recruited into the outer retina following PD (B). This is reduced following 670 nm treatment at 0 days (PD + R0, C), 3 days (PD + R3, D) and 14 days (PD + R14, E). Inserts in each panel show that the majority of microglia in the outer retina are activated as evidenced by their amoeboid appearance. F-G: Whole retinal (F) and outer retinal (G) IBA1+ cell counts show that this reduction is significant at 0 days and 3 days. GCL, ganglion cell layer; INL, inner nuclear layer; outer nuclear layer; IHC, immunohistochemistry. All data is presented as the mean \pm SEM. * denotes P < .05 and N = 7-10 for all groups. (For interpretation of the references to color in this figure legend, the reader is referred to the Web version of this article.)

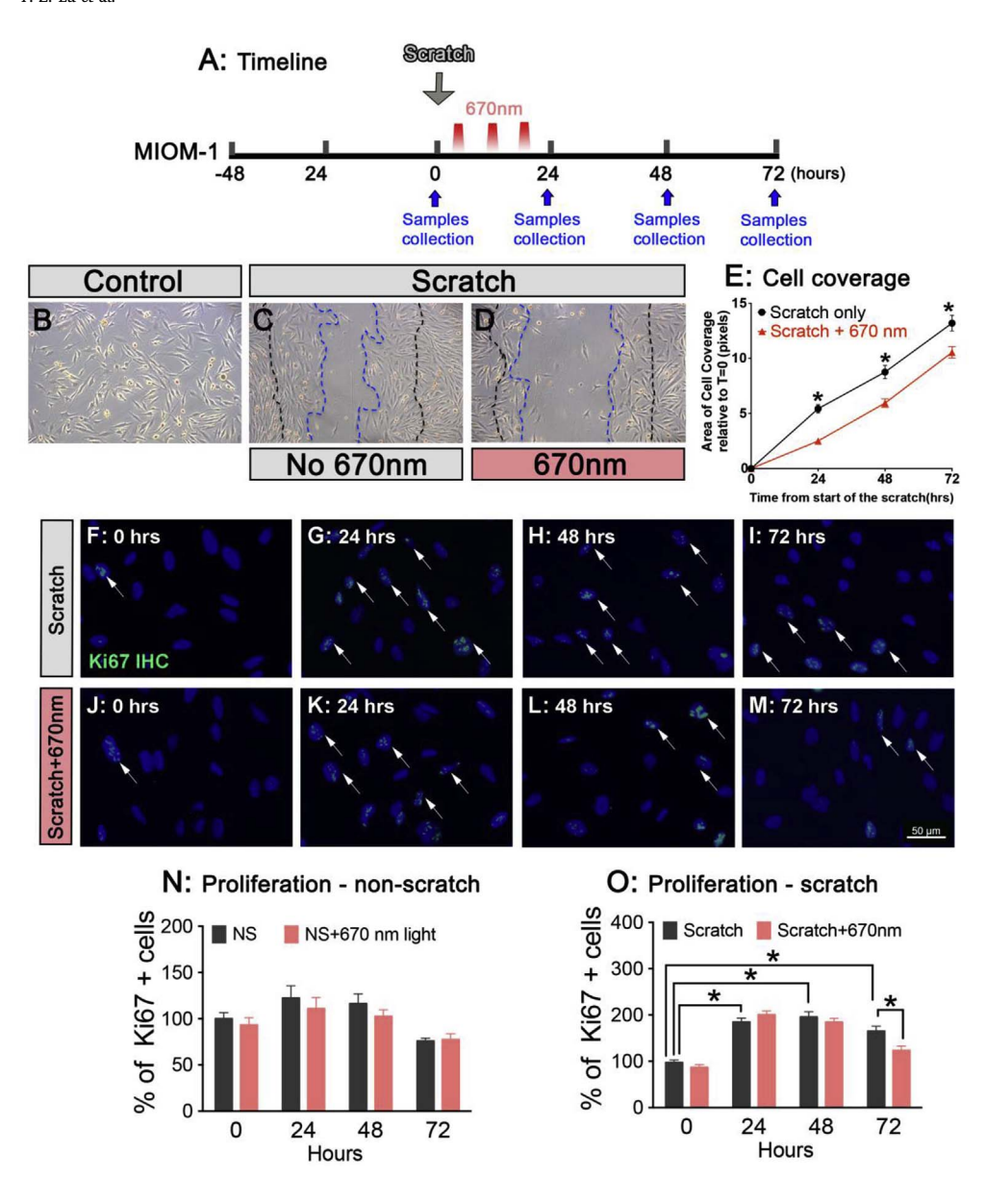


Fig. 5. Wound coverage and proliferation following 670 nm light treatment in an in vitro scratch model. A: Experimental paradigm using the human Müller cell line MIO-M1. B-D: Representative images show control cells (B), cells at 72 h following the scratch (C) and cells at 72 h after the scratch and 670 nm light treatment (D). E: Quantification of scratch coverage shows that 670 nm light significantly reduces the rate of area coverage at each time point. F-M: Ki67 immunohistochemistry (IHC) shows that mitosis increases in MIO-M1 cells following the scratch injury, and this rate persists for up to 72 h (F-I), whereas cells treated with 670 nm light have a reduced expression of Ki67 Proliferation in non-scratched groups (NS, NS +670) showed no difference over the time course or with 670 nm light treatment. O: Quantification of Ki67 + cells showed an upregulation of proliferation following the scratch injury, and a reduction in cells treated with 670 nm light. All data is presented as the mean + SEM, * denotes P < .05 and experiments were performed with N = 3 in biological triplicate. Scale bar represents 50 µm.

reduced the rate of area coverage significantly at each time point (Fig. 5E). Within 24 h, the area covered in the non-treated (S) wells was approximately double (2.26 \pm 0.16 pixels/hour) that of the treated (S +670) wells (1.04 \pm 0.13 pixels/hour), representing a significant slowing of motility by PBM (P < .05, Fig. 5E). After the first 24 h, when 670 nm light treatment ceased, the rate of area coverage was almost identical in the two groups (1.62 \pm 0.08 pixels/hour in the S group and 1.67 \pm 0.09 pixels/hour in the S+670 group, P > .05). These data suggest that the reduction of area coverage occurred within the duration of 670 nm light treatment. The difference in area coverage remained significantly different between the two groups up to 72 h (Fig. 5E).

To investigate whether MCs displayed proliferative gliosis in this model, we used Ki67, a known proliferation marker. The number of Ki67 + cells between the Non-scratch (NS) and the NS+670 groups did not differ over 72 h (Fig. 5N). Ki67 labelling was present in MIO-M1 cellular nuclei at 24 h post-injury (S group), and this represented a significant increase when compared to T=0 (P < .05, Fig. 5F-I, O). The number of proliferating cells remained high compared to controls, with no significant difference observed between 24, 48 and 72 h (Fig. 5F-I, O). In the S+670 group, the number of proliferating cells were comparable to those in the S group in the early stages (within

48 h) following the scratch. However, at 72 h 670 nm light-treated cells showed significantly less mitosis compared to the S group (P < .05, Fig. 5I, M, O).

3.5. 670 nm light treatment reduced cell death after injury in vitro

We used flow cytometry to confirm whether the reduction in mitotic cell numbers following 670 nm light treatment was related to MC cycle status or cell death. We calculated the percentage of cells in the G0/G1, G2/M and S phases (Fig. 6A–C) and found no significant differences between 670 nm light-treated and non-treated groups at any of the time points examined. The reduction in the G2/M phase population observed at 24 h in the treated group did not reach significance, when compared to non-treated cells at the same time (Fig. 6B). MMC significantly slowed the rate of area coverage in non-treated cells (Fig. 6D, dashed black line); however, it had no effect on 670 nm light-treated cells (Fig. 6D, red lines). The percentage of dead cells in all groups was low (\sim 2–3%), during the time period observed (Fig. 6E). Notably, the percentage of dead cells at 24 and 48 h were significantly lower in the 670 nm light-treated scratch group (S+670) compared to the control scratch group (S) over the same time course (Fig. 6E).

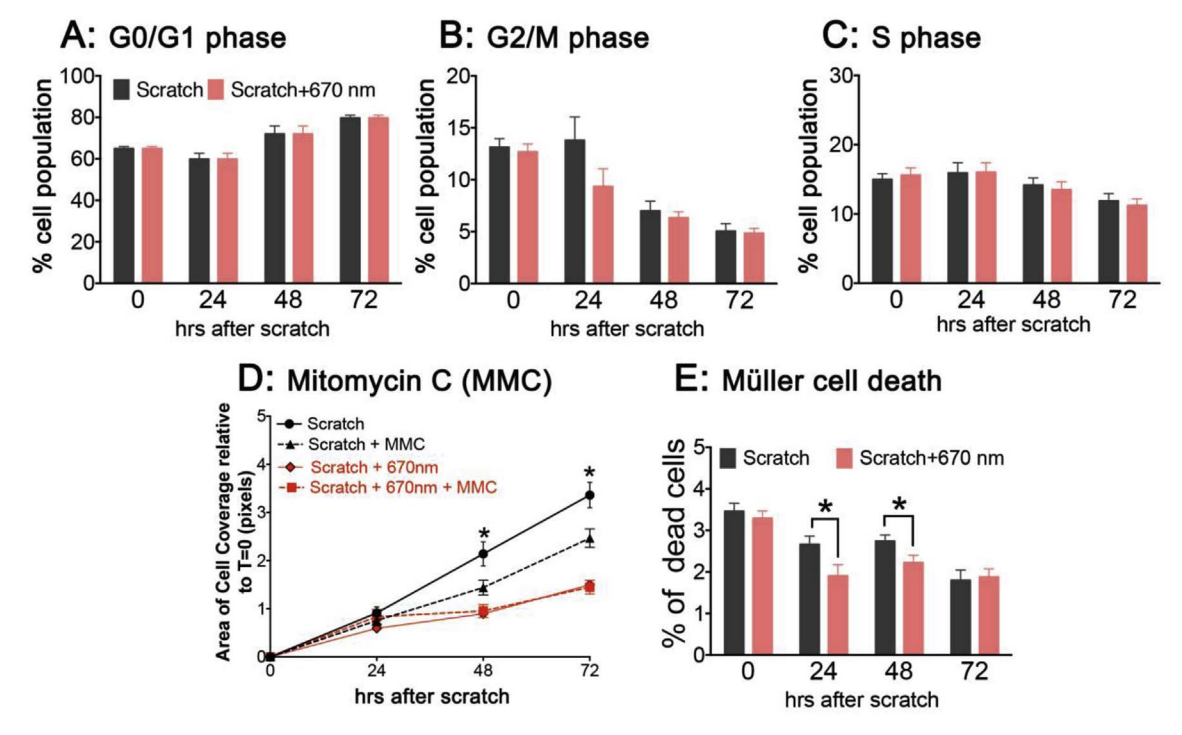


Fig. 6. Effects of 670 nm light treatment on MC cell cycle status and cell death following the scratch. A-C: The population of MIO-M1 cells at each phase of the cell cycle was analysed by flow cytometry, and it was found that there were no differences between 670 nm treated and non-treated groups across the time course for the G0/G1 phase (A), G2/M phase (B) and the S phase (C). D: Mitomycin C (MMC) pre-treatment of cells prior to the scratch injury significantly reduced the rate of area coverage in non-670-treated cells (dashed black line) but did not have an effect on 670 nm light-treated cells (red lines). E: 670 nm light treatment reduced the percentage of dead cells at 24 and 48 h compared to scratch controls. All data is presented as the mean \pm SEM. * denotes P < .05 and experiments were performed with N = 3 in biological triplicate. (For interpretation of the references to color in this figure legend, the reader is referred to the Web version of this article.)

3.6. Effect of 670 nm light treatment on cell spreading and migration

To assess differences in MC size, we used vimentin and nucleic acid labelling to visualize the cytoplasm and nucleus of cells at the edge of the scratch site (Fig. 7A–H). The area of cytoplasm was significantly increased at 24 h and was maintained at 48 and 72 h following the mechanical scratch (Fig. 7A–D, I). Cells treated with 670 nm light

showed no significant change in cell area between time points (Fig. 7E–H, I). The ratio of cytoplasm to nuclear area was significantly higher in the non-treated group at all time points compared to the $670 \, \text{nm}$ light-treated group following scratch, suggesting that $670 \, \text{nm}$ light treatment suppressed cell spreading (P < .05, Fig. 7I).

To assess the effect of 670 nm light treatment on MC migration, transwell chambers were used. Only a few migrating cells were noted in

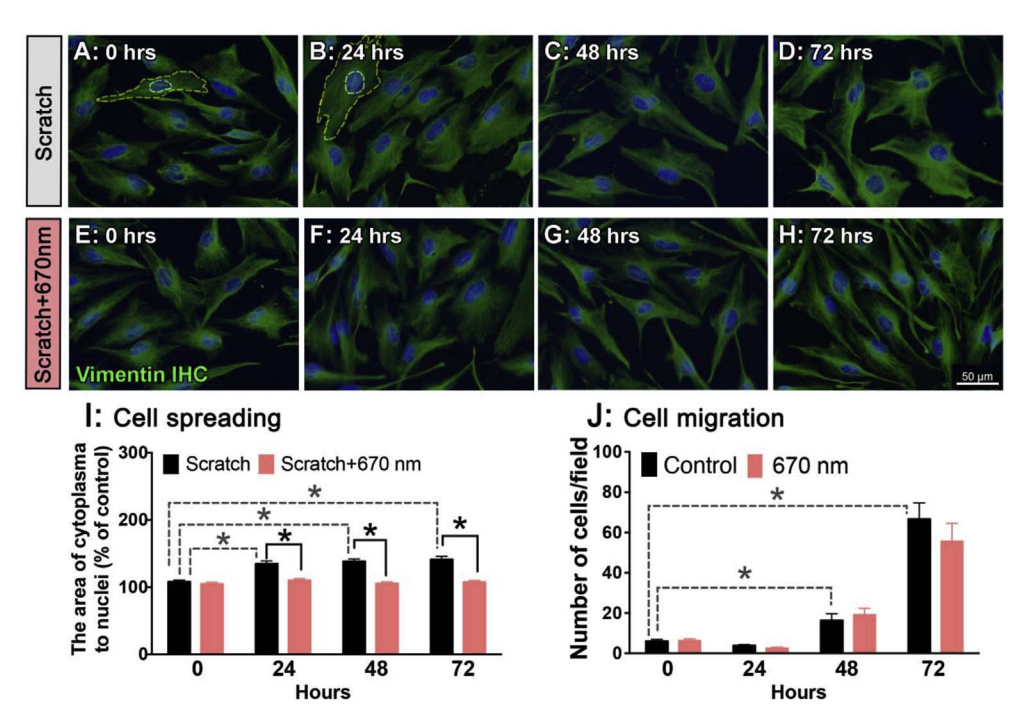


Fig. 7. Cell spreading of MIO-M1 cells was modified by 670 nm light treatment. A-H: Vimentin immunocytochemistry (ICC, green) and cell nuclei staining (bisbenzimide, blue) allowed the measurement of the area of the cytoplasm and the area of nucleus (yellow dashed lines). I: Quantification of the ratio of the cytoplasmic area to the nuclear area showed that there was a significant decrease in cell spreading following 670 nm light treatment. J: Cell migratory capability across a membrane of the transwell was measured as the number of cells per field. Although cell migration increased across the time course, 670 nm light did not have an effect on the migratory capacity of MIO-M1cells. All data is presented as the mean ± SEM. * denotes P < .05 and experiments were performed with N = 3 in biological triplicate. Scale bar represents 50 µm. (For interpretation of the references to color in this figure legend, the reader is referred to the Web version of this article.)

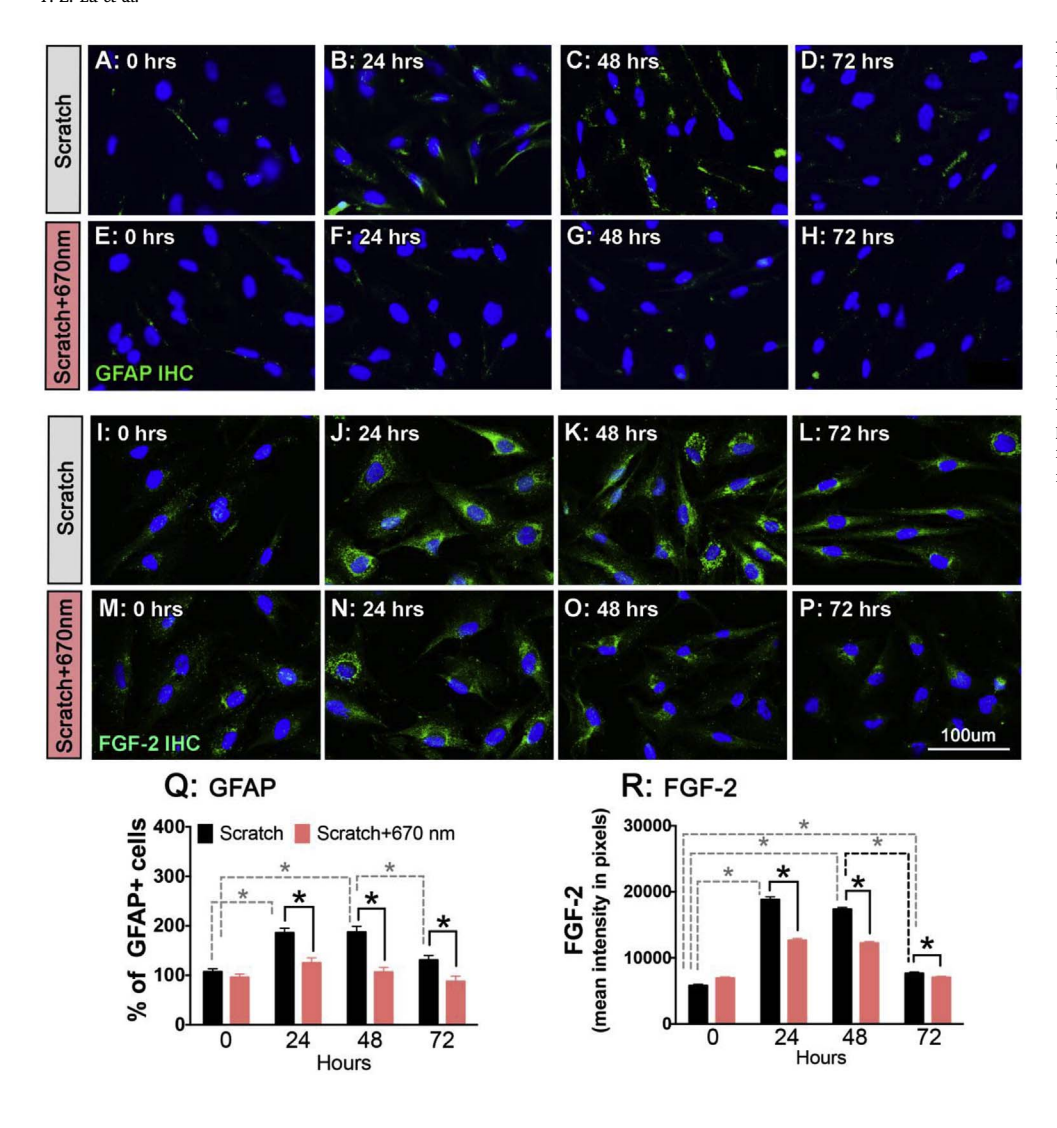


Fig. 8. The effects of 670 nm light treatment on Müller cell stress. A-H: MIO-M1 cells were labeled with GFAP (ICC, green), which increased following the scratch injury (A-D). Treatment with 670 nm light reduced the expression of GFAP (E-H). I-P: MIO-M1 cells were labeled for FGF-2 (green), which also increased in the scratch model (I-L). Treatment with 670 nm light reduced FGF-2 expression (M-P). Q-R: Quantification of GFAP (Q) and FGF-2 (R) labelling showed that 670 nm light treatment significantly reduced GFAP and FGF-2 across the time course following the scratch injury. All data is presented as the mean ± SEM. * denotes P < .05 and experiments were performed with N = 3 in biological triplicate. Scale bar represents 100 µm. (For interpretation of the references to color in this figure legend, the reader is referred to the Web version of this article.)

the first 24 h, but a significant increase in migration was observed at 48 h in both groups when compared to T = 0 (P < .05, Fig. 7J). A further significant increase in migration was present at 72 h in both groups compared to T = 48 (P < .05, Fig. 7J). There was no significant difference in the number of migrating cells between 670 nm light-treated and non-treated groups, suggesting that 670 nm light did not have an impact on the migratory ability of MCs (P > .05, Fig. 7J).

3.7. Assessment of cell stress in vitro

To assess cell stress status in MIO-M1 cells in the scratch model, GFAP (Fig. 8A–H) and FGF-2 (Fig. 8I-P) immunolabelling were performed. In the S group, the percentage of GFAP + cells at the scratch site significantly increased following injury compared to T=0 (Fig. 8A–D, Q). The increased GFAP labelling was maintained thereafter, but by 72 h, there was a significant reduction in GFAP + cells compared to T=48 (Fig. 8A–D, Q). Treatment with 670 nm light significantly reduced GFAP at all time points (P < .05, Fig. 8E–H, Q).

MCs expressed FGF-2 in the cellular cytoplasm immediately after injury (Fig. 8I-P, R). A significant increase in FGF-2 expression was apparent in the cytoplasm in the S group at 24 and 48 h compared to T=0 (P < .05, Fig. 8J, K, R). Notably, more intense fluorescence was observed around the nucleus. By 72 h, FGF-2 labelling subsided but was still higher than at T=0 levels (P < .05, Fig. 8L, R). In the S+670 group, FGF-2 expression increased following injury, however this was significantly less than the S group across the time course (P < .05, Fig. 8M-P, R). Collectively, these data suggest that 670 nm light

treatment can mitigate cell stress caused by mechanical injury.

4. Discussion

In this study, we demonstrated the effects of 670 nm light treatment on activated MCs using *in vivo* and *in vitro* models of retinal injury. We have demonstrated that treatment with 670 nm light can modulate the activation of MCs following injury, and thereby leading to a reduction 1) in MG/M Φ recruitment into the outer retina, 2) in retinal inflammation 3) MC proliferation and migration, and therefore a mitigation of glial scar formation, which ultimately result in increased photoreceptor survivability. We also show that it is critical to commence treatment shortly after injury in order to maximise these beneficial effects.

4.1. Early 670 nm light treatment mitigates MC reactive gliosis

The initial response of MCs following injury is through reactive gliosis which includes the structural changes of these cells, the increased presence of cytoskeletal proteins (GFAP, Vimentin) indicating increased cell stress, the upregulation of neuroprotective factors (FGF-2) and the production of pro-inflammatory cytokines (Ccl2, IL-1b) (Rutar et al., 2010, 2011). We have previously shown that treatment with 670 nm light prior to retinal injury mitigates photoreceptor loss, and MC activation (Albarracin and Valter, 2012).

In the current study, 670 nm light treatment commenced after activation of MCs, and we demonstrate that early treatment with 670 nm

light reduced retinal cell stress decreased pro-inflammatory cytokine expression and reduced the recruitment of MG/M Φ following PD, when treatment commenced 0–3 days post-injury. Furthermore, we show that 670 nm treatment can still partially prevent photoreceptor loss and reduce the progression of the retinal lesion when treatment commence early after retinal injury (0–3 days), however later treatment (14 days) does not produce any measurable benefit for photoreceptor survival.

4.2. Effect of 670 nm light treatment on MC migration: implications for glial scarring

Previous studies reported that following retinal detachment, MC nuclei migrate into the damaged outer retina and undergo mitosis thereby forming subretinal glial scars (Lewis et al., 1999, 2010), and suggesting that movement and proliferation of MC nuclei is relevant to glial scar formation. In the present study, we found that in the area of the lesion there was evidence of glial scar formation within and outside of the ONL in all retinas, confirming previous reports (REF), however, those that were treated with 670 nm light showed a much less robust scarring. Our in vitro findings show that 670 nm light treatment of MCs reduced cell spreading, mitosis and FGF-2 expression. FGF-2 has been shown to induce GFAP expression in MCs, and this has been linked to glial scar formation in a rabbit retinal detachment model (Lewis et al., 1992). In addition, MC migration is regulated by matrix metalloprotease (MMP) and protease inhibitor α_2 -macroglobulin (α_2 M) (Barcelona et al., 2011, 2013; Limb et al., 2002a). $\alpha_2 M$ has been implicated in the induction of GFAP expression in MCs (Barcelona et al., 2011, 2013). 670 nm light treatment has been shown to reduce MMP expression in wound healing of diabetic rats (Aparecida Da Silva et al., 2013). Therefore, the decreased GFAP expression observed in our treatment model may be related to changes in MMP or α₂M expression in activated MCs, which might regulate cellular migration as well as a downstream effect of the reduction in FGF-2 expression. Further studies exploring the association between MMP activity in MCs and 670 nm irradiation are required however to prove this association.

Nakazawa et al., using transgenic mice models have shown that the absence of GFAP and Vimentin can effectively attenuate MC gliosis and subsequently limit photoreceptor death following retinal detachment (Nakazawa et al., 2007b). Therefore, the reduction of MC activation, and mitigated levels of GFAP and Vimentin in 670 nm light-treated retinas may be strongly associated with the higher photoreceptor survivability and the slowing of the progression of retinal lesion, observed in the present study.

4.3. 670 nm light treatment mitigates retinal inflammation following injury

There is an early and rapid increase in *Ccl2* expression in activated MCs following PD, leading to the recruitment of MG/MΦ into the damaged photoreceptor layer (Rutar et al., 2012b, 2011, 2010). The present study demonstrated that 670 nm light-treated retinas had less MG/MΦ recruitment following PD, which is consistent with previous studies (Albarracin et al., 2011; Begum et al., 2013; Kokkinopoulos, 2013; Kokkinopoulos et al., 2013). Previously we reported that the recruitment of MG/MΦ is directly related to the Ccl2 expression in MC (Rutar et al., 2012b). Although, the current study shows no effects of 670 nm light on *Ccl2* expression in the retina, it is possibly due to the early, rapid and transient regulation of *Ccl2* expression, and may not be observable at this time point (30 days post injury). However, the observed reduction of MG/MΦ in the outer retina suggests that 670 nm light has an effect on the recruitment of immune cells into the retina.

Inflammasomes have been implicated in retinal degenerations (Kauppinen et al., 2016). This study demonstrates that 670 nm light-treated retinas had a reduced expression of a number of inflammasome-related genes following PD, including $Il-1\beta$, Nlrp3 and Casp8. It has been reported that MCs express IL-1 β when incubated with activated microglia, when grown under hyperglycemic conditions, or when co-

cultured with degenerated photoreceptors (Liu et al., 2012; Lu et al., 2017; Wang et al., 2011). These activated MCs can then stimulate MG/M Φ to produce pro-inflammatory cytokines and complement proteins, leading to further retinal damage (Fernando et al., 2016; Natoli et al., 2017). The reduction of inflammasome-related genes observed in the current study following 670 nm light treatment may be due to decreased MC activation. However, it is thought that the primary producers of retinal inflammasomes are the RPE cells and MG/M Φ (Astray et al., 2016). Although inflammasome activation has been shown previously in the MC line under hyperglycemic conditions (Trueblood et al., 2011), it is thought that the effect of 670 nm light on the inflammasome could be due to other retinal cell types. Further investigation into the role of MCs in inflammasome activation is necessary.

4.4. Mechanism of 670 nm light treatment on Müller cells

Although the exact mechanism by which 670 nm light affects tissue is still debated, it has been proposed that this wavelength of light is most likely absorbed by cytochrome c oxidase (COX) (Karu, 1999, 2008), a rate-limiting enzyme in terminal phosphorylation in the mitochondrial respiratory chain, leading to increased COX expression (Begum et al., 2013) and elevated mitochondrial membrane potential (Kokkinopoulos et al., 2013), which is proportional to mitochondrial ATP production (Wong-Riley et al., 2005). ATP can be released from MCs into the extracellular space upon osmotic stress and glutamate stimulation (Voigt et al., 2015). Extracellular ATP and its downstream signaling cascade have been reported to inhibit MC swelling, an indication of MC gliosis, under hypo-osmotic conditions (Uckermann et al., 2006). Consequently, 670 nm light may trigger MCs to release ATP into the extracellular space under stress, which subsequently contribute to maintaining retinal homeostasis.

Karu and Kolyakov have demonstrated that far-red light (667.5 nm-683.7 nm) facilitate the synthesis of DNA and RNA in HeLa cells (Karu and Kolyakov, 2005), suggesting that these wavelength of lights can directly modify gene expression. We previously showed that 670 nm irradiation changed gene expressions in control and PD rat retinas (Natoli et al., 2010). The modulated genes included non-coding RNAs (miRNA) as well as genes coding complement (Rutar et al., 2012a), neuroprotective (Albarracin and Valter, 2012), and oxidative stress-related (Albarracin et al., 2013) proteins. These investigations suggest that 670 nm light may influence gene expression by regulating their transcription, thereby mitigating damage.

5. Conclusion

Our data support the use of 670 nm light treatment in retinal conditions where MC activation is a key feature, such as AMD, diabetic retinopathy and retinal detachment. These results are encouraging, as they show that irradiation with 670 nm light may be beneficial when commenced after the onset of disease.

Acknowledgments

This work was supported by the Australian Government National Health and Medical Research Council Grant (APP1049990), the Australian Government Research Training Program and the Gretel and Gordon Bootes Foundation.

References

Albarracin, R., Eells, J., Valter, K., 2011. Photobiomodulation protects the retina from light-induced photoreceptor degeneration. Invest. Ophthalmol. Vis. Sci. 52, 3582–3592

Albarracin, R., Natoli, R., Rutar, M., Valter, K., Provis, J., 2013. 670 nm light mitigates oxygen-induced degeneration in C57BL/6J mouse retina. BMC Neurosci. 14, 125. Albarracin, R., Valter, K., 2012. 670 nm red light preconditioning supports Muller cell

- function: evidence from the white light-induced damage model in the rat retina. Photochem. Photobiol. $88,\,1418-1427.$
- Aparecida Da Silva, A., Leal-Junior, E.C., Alves, A.C., Rambo, C.S., Dos Santos, S.A., Vieira, R.P., De Carvalho Pde, T., 2013. Wound-healing effects of low-level laser therapy in diabetic rats involve the modulation of MMP-2 and MMP-9 and the redistribution of collagen types I and III. J. Cosmet. Laser Ther.: Official Pub. Eur. Soc. Laser Dermatol. 15, 210–216.
- Arranz-Valsero, I., Soriano-Romani, L., Garcia-Posadas, L., Lopez-Garcia, A., Diebold, Y., 2014. IL-6 as a corneal wound healing mediator in an in vitro scratch assay. Exp. Eye Res. 125. 183–192.
- Astray, G., Soto, B., Lopez, D., Iglesias, M.A., Mejuto, J.C., 2016. Application of transit data analysis and artificial neural network in the prediction of discharge of Lor River, NW Spain. Water Sci. Technol.: J. Int. Assoc. Water Pollut. Res. 73, 1756–1767.
- Barcelona, P.F., Jaldin-Fincati, J.R., Sanchez, M.C., Chiabrando, G.A., 2013. Activated alpha2-macroglobulin induces Muller glial cell migration by regulating MT1-MMP activity through LRP1. Faseb. J.: Official Pub. Fed. Am. Soc. Exp. Biol. 27, 3181-3197
- Barcelona, P.F., Ortiz, S.G., Chiabrando, G.A., Sanchez, M.C., 2011. alpha2-Macroglobulin induces glial fibrillary acidic protein expression mediated by lowdensity lipoprotein receptor-related protein 1 in Muller cells. Invest. Ophthalmol. Vis. Sci. 52, 778–786.
- Begum, R., Powner, M.B., Hudson, N., Hogg, C., Jeffery, G., 2013. Treatment with 670 nm light up regulates cytochrome C oxidase expression and reduces inflammation in an age-related macular degeneration model. PLoS One 8, e57828.
- Bringmann, A., Iandiev, I., Pannicke, T., Wurm, A., Hollborn, M., Wiedemann, P., Osborne, N.N., Reichenbach, A., 2009. Cellular signaling and factors involved in Muller cell gliosis: neuroprotective and detrimental effects. Prog. Retin. Eye Res. 28, 423–451.
- Bringmann, A., Wiedemann, P., 2012. Muller glial cells in retinal disease. Ophthalmologica. Journal international d'ophtalmologie. International journal of ophthalmology. Zeitschrift fur Augenheilkunde 227, 1–19.
- Calaza, K.C., Kam, J.H., Hogg, C., Jeffery, G., 2015. Mitochondrial decline precedes phenotype development in the complement factor H mouse model of retinal degeneration but can be corrected by near infrared light. Neurobiol. Aging 36, 2869–2876.
- Conlan, M.J., Rapley, J.W., Cobb, C.M., 1996. Biostimulation of wound healing by low-energy laser irradiation. A review. J. Clin. Periodontol. 23, 492–496.
- Desmet, K.D., Paz, D.A., Corry, J.J., Eells, J.T., Wong-Riley, M.T., Henry, M.M., Buchmann, E.V., Connelly, M.P., Dovi, J.V., Liang, H.L., Henshel, D.S., Yeager, R.L., Millsap, D.S., Lim, J., Gould, L.J., Das, R., Jett, M., Hodgson, B.D., Margolis, D., Whelan, H.T., 2006. Clinical and experimental applications of NIR-LED photobiomodulation. Photomed. Laser Surg, 24, 121–128.
- Eells, J.T., Henry, M.M., Summerfelt, P., Wong-Riley, M.T., Buchmann, E.V., Kane, M., Whelan, N.T., Whelan, H.T., 2003. Therapeutic photobiomodulation for methanolinduced retinal toxicity. Proc. Natl. Acad. Sci. U.S.A. 100, 3439–3444.
- Fernando, N., Natoli, R., Valter, K., Provis, J., Rutar, M., 2016. The broad-spectrum chemokine inhibitor NR58-3.14.3 modulates macrophage-mediated inflammation in the diseased retina. J. Neuroinflammation 13, 47.
- Fitzgerald, M., Hodgetts, S., Van Den Heuvel, C., Natoli, R., Hart, N.S., Valter, K., Harvey, A.R., Vink, R., Provis, J., Dunlop, S.A., 2013. Red/near-infrared irradiation therapy for treatment of central nervous system injuries and disorders. Rev. Neurosci. 24, 205–226
- Giacci, M.K., Wheeler, L., Lovett, S., Dishington, E., Majda, B., Bartlett, C.A., Thornton, E., Harford-Wright, E., Leonard, A., Vink, R., Harvey, A.R., Provis, J., Dunlop, S.A., Hart, N.S., Hodgetts, S., Natoli, R., Van Den Heuvel, C., Fitzgerald, M., 2014. Differential effects of 670 and 830 nm red near infrared irradiation therapy: a comparative study of optic nerve injury, retinal degeneration, traumatic brain and spinal cord injury. PLoS One 9, e104565.
- Herranz-Aparicio, J., Vazquez-Delgado, E., Arnabat-Dominguez, J., Espana-Tost, A., Gay-Escoda, C., 2013. The use of low level laser therapy in the treatment of temporomandibular joint disorders. Review of the literature. Med. Oral, Patol. Oral Cirugía Bucal 18, e603–612.
- Ivandic, B.T., Ivandic, T., 2008. Low-level laser therapy improves vision in patients with age-related macular degeneration. Photomed. Laser Surg. 26, 241–245.
- Ivandic, B.T., Ivandic, T., 2012. Low-level laser therapy improves visual acuity in adolescent and adult patients with amblyopia. Photomed. Laser Surg. 30, 167–171.
- Karu, T., 1999. Primary and secondary mechanisms of action of visible to near-IR radiation on cells. J. Photochem. Photobiol. B Biol. 49, 1–17.
- Karu, T.I., 2008. Mitochondrial signaling in mammalian cells activated by red and near-IR radiation. Photochem. Photobiol. 84, 1091–1099.
- Karu, T.I., Kolyakov, S.F., 2005. Exact action spectra for cellular responses relevant to phototherapy. Photomed. Laser Surg. 23, 355–361.
- Kauppinen, A., Paterno, J.J., Blasiak, J., Salminen, A., Kaarniranta, K., 2016.
 Inflammation and its role in age-related macular degeneration. Cell. Mol. Life Sci.:
 CMLS 73, 1765–1786.
- Kokkinopoulos, I., 2013. 670 nm LED ameliorates inflammation in the CFH(-/-) mouse neural retina. J. Photochem. Photobiol. B Biol. 122, 24–31.
- Kokkinopoulos, I., Colman, A., Hogg, C., Heckenlively, J., Jeffery, G., 2013. Age-related retinal inflammation is reduced by 670 nm light via increased mitochondrial membrane potential. Neurobiol. Aging 34, 602–609.
- Lawrence, J.M., Singhal, S., Bhatia, B., Keegan, D.J., Reh, T.A., Luthert, P.J., Khaw, P.T., Limb, G.A., 2007. MIO-M1 cells and similar muller glial cell lines derived from adult human retina exhibit neural stem cell characteristics. Stem Cell. 25, 2033–2043.
- Lewis, G., Mervin, K., Valter, K., Maslim, J., Kappel, P.J., Stone, J., Fisher, S., 1999. Limiting the proliferation and reactivity of retinal Muller cells during experimental retinal detachment: the value of oxygen supplementation. Am. J. Ophthalmol. 128, 165-172.

- Lewis, G.P., Chapin, E.A., Luna, G., Linberg, K.A., Fisher, S.K., 2010. The fate of Muller's glia following experimental retinal detachment: nuclear migration, cell division, and subretinal glial scar formation. Mol. Vis. 16, 1361–1372.
- Lewis, G.P., Erickson, P.A., Guerin, C.J., Anderson, D.H., Fisher, S.K., 1992. Basic fibroblast growth factor: a potential regulator of proliferation and intermediate filament expression in the retina. J. Neurosci.: Official J. Soc. Neurosci. 12, 3968–3978.
- Limb, G.A., Daniels, J.T., Pleass, R., Charteris, D.G., Luthert, P.J., Khaw, P.T., 2002a.
 Differential expression of matrix metalloproteinases 2 and 9 by glial Muller cells: response to soluble and extracellular matrix-bound tumor necrosis factor-alpha. Am. J. Pathol. 160, 1847–1855.
- Limb, G.A., Salt, T.E., Munro, P.M., Moss, S.E., Khaw, P.T., 2002b. In vitro characterization of a spontaneously immortalized human Muller cell line (MIO-M1). Invest. Ophthalmol. Vis. Sci. 43, 864–869.
- Liu, Y., Biarnes Costa, M., Gerhardinger, C., 2012. IL-1beta is upregulated in the diabetic retina and retinal vessels: cell-specific effect of high glucose and IL-1beta autostimulation. PLoS One 7, e36949.
- Lu, Q., Jiang, Y.R., Qian, J., Tao, Y., 2013. Apelin-13 regulates proliferation, migration and survival of retinal Muller cells under hypoxia. Diabetes Res. Clin. Pract. 99, 158–167.
- Lu, Y.Z., Natoli, R., Madigan, M., Fernando, N., Saxena, K., Aggio-Bruce, R., Jiao, H., Provis, J., Valter, K., 2017. Photobiomodulation with 670 nm light ameliorates Muller cell-mediated activation of microglia and macrophages in retinal degeneration. Exp. Eye Res. 165, 78–89.
- Matsushima, K., Larsen, C.G., DuBois, G.C., Oppenheim, J.J., 1989. Purification and characterization of a novel monocyte chemotactic and activating factor produced by a human myelomonocytic cell line. J. Exp. Med. 169, 1485–1490.
- Merry, G.F., Munk, M.R., Dotson, R.S., Walker, M.G., Devenyi, R.G., 2017.
 Photobiomodulation reduces drusen volume and improves visual acuity and contrast sensitivity in dry age-related macular degeneration. Acta Ophthalmol. 95, e270–e277.
- Nakazawa, T., Hisatomi, T., Nakazawa, C., Noda, K., Maruyama, K., She, H., Matsubara, A., Miyahara, S., Nakao, S., Yin, Y., Benowitz, L., Hafezi-Moghadam, A., Miller, J.W., 2007a. Monocyte chemoattractant protein 1 mediates retinal detachment-induced photoreceptor apoptosis. Proc. Natl. Acad. Sci. U.S.A. 104, 2425–2430.
- Nakazawa, T., Takeda, M., Lewis, G.P., Cho, K.S., Jiao, J., Wilhelmsson, U., Fisher, S.K., Pekny, M., Chen, D.F., Miller, J.W., 2007b. Attenuated glial reactions and photoreceptor degeneration after retinal detachment in mice deficient in glial fibrillary acidic protein and vimentin. Invest. Ophthalmol. Vis. Sci. 48, 2760–2768.
- Natoli, R., Fernando, N., Madigan, M., Chu-Tan, J.A., Valter, K., Provis, J., Rutar, M., 2017. Microglia-derived IL-1β promotes chemokine expression by Müller cells and RPE in focal retinal degeneration. Mol. Neurodegener. 12, 31.
- Natoli, R., Valter, K., Barbosa, M., Dahlstrom, J., Rutar, M., Kent, A., Provis, J., 2013. 670nm photobiomodulation as a novel protection against retinopathy of prematurity: evidence from oxygen induced retinopathy models. PLoS One 8, e72135.
- Natoli, R., Zhu, Y., Valter, K., Bisti, S., Eells, J., Stone, J., 2010. Gene and noncoding RNA regulation underlying photoreceptor protection: microarray study of dietary antioxidant saffron and photobiomodulation in rat retina. Mol. Vis. 16, 1801–1822.
- Romo, P., Madigan, M.C., Provis, J.M., Cullen, K.M., 2011. Differential effects of TGF-beta and FGF-2 on in vitro proliferation and migration of primate retinal endothelial and Muller cells. Acta Ophthalmol. 89, e263–268.
- Rutar, M., Natoli, R., Albarracin, R., Valter, K., Provis, J., 2012a. 670-nm light treatment reduces complement propagation following retinal degeneration. J. Neuroinflammation 9, 257.
- Rutar, M., Natoli, R., Provis, J.M., 2012b. Small interfering RNA-mediated suppression of Ccl2 in Muller cells attenuates microglial recruitment and photoreceptor death following retinal degeneration. J. Neuroinflammation 9, 221.
- Rutar, M., Natoli, R., Valter, K., Provis, J.M., 2011. Early focal expression of the chemokine Ccl2 by Muller cells during exposure to damage-inducing bright continuous light. Invest. Ophthalmol. Vis. Sci. 52, 2379–2388.
- Rutar, M., Provis, J.M., Valter, K., 2010. Brief exposure to damaging light causes focal recruitment of macrophages, and long-term destabilization of photoreceptors in the albino rat retina. Curr. Eye Res. 35, 631–643.
- Shen, W., Fruttiger, M., Zhu, L., Chung, S.H., Barnett, N.L., Kirk, J.K., Lee, S., Coorey, N.J., Killingsworth, M., Sherman, L.S., Gillies, M.C., 2012. Conditional Mullercell ablation causes independent neuronal and vascular pathologies in a novel transgenic model. J. Neurosci.: Official J. Soc. Neurosci. 32, 15715–15727.
- Tang, J., Du, Y., Lee, C.A., Talahalli, R., Eells, J.T., Kern, T.S., 2013. Low-intensity far-red light inhibits early lesions that contribute to diabetic retinopathy: in vivo and in vitro. Invest. Ophthalmol. Vis. Sci. 54, 3681–3690.
- Tang, J., Herda, A.A., Kern, T.S., 2014. Photobiomodulation in the treatment of patients with non-center-involving diabetic macular oedema. Br. J. Ophthalmol. 98, 1013–1015
- Trueblood, K.E., Mohr, S., Dubyak, G.R., 2011. Purinergic regulation of high-glucose-induced caspase-1 activation in the rat retinal Muller cell line rMC-1. American journal of physiology. Cell Physiol. 301, C1213–C1223.
- Uckermann, O., Wolf, A., Kutzera, F., Kalisch, F., Beck-Sickinger, A.G., Wiedemann, P., Reichenbach, A., Bringmann, A., 2006. Glutamate release by neurons evokes a purinergic inhibitory mechanism of osmotic glial cell swelling in the rat retina: activation by neuropeptide Y. J. Neurosci. Res. 83, 538–550.
- Valter, K., Bisti, S., Gargini, C., Di Loreto, S., Maccarone, R., Cervetto, L., Stone, J., 2005. Time course of neurotrophic factor upregulation and retinal protection against light-induced damage after optic nerve section. Invest. Ophthalmol. Vis. Sci. 46, 1748–1754.
- Voigt, J., Grosche, A., Vogler, S., Pannicke, T., Hollborn, M., Kohen, L., Wiedemann, P., Reichenbach, A., Bringmann, A., 2015. Nonvesicular release of ATP from rat retinal glial (Muller) cells is differentially mediated in response to osmotic stress and

- glutamate. Neurochem. Res. 40, 651-660.
- Wang, M., Ma, W., Zhao, L., Fariss, R.N., Wong, W.T., 2011. Adaptive Muller cell responses to microglial activation mediate neuroprotection and coordinate inflammation in the retina. J. Neuroinflammation 8, 173.
- Whelan, H.T., Smits Jr., R.L., Buchman, E.V., Whelan, N.T., Turner, S.G., Margolis, D.A., Cevenini, V., Stinson, H., Ignatius, R., Martin, T., Cwiklinski, J., Philippi, A.F., Graf, W.R., Hodgson, B., Gould, L., Kane, M., Chen, G., Caviness, J., 2001. Effect of NASA light-emitting diode irradiation on wound healing. J. Clin. Laser Med. Surg. 19,
- 305-314.
- Wong-Riley, M.T., Liang, H.L., Eells, J.T., Chance, B., Henry, M.M., Buchmann, E., Kane, M., Whelan, H.T., 2005. Photobiomodulation directly benefits primary neurons functionally inactivated by toxins: role of cytochrome c oxidase. J. Biol. Chem. 280, 4761–4771.
- Yoshimura, T., Robinson, E.A., Tanaka, S., Appella, E., Kuratsu, J., Leonard, E.J., 1989.Purification and amino acid analysis of two human glioma-derived monocyte chemoattractants. J. Exp. Med. 169, 1449–1459.